Received: 2 November 2020 | Revised: 25 November 2020 | Accepted: 30 November 2020

DOI: 10.1111/cts.12962

ARTICLE

Altered vitamin A metabolism in human liver slices corresponds to fibrogenesis

Lindsay C. Czuba[1] | Xia Wu[2] | Weize Huang[1] | Nicole Hollingshead[2] | Jessica B. Roberto[2] | Heidi L. Kenerson[3] | Raymond S. Yeung[3] | Ian N. Crispe[2] | Nina Isoherranen[1]

[1]Department of Pharmaceutics, University of Washington, Seattle, Washington, USA

[2]Department of Laboratory Medicine and Pathology, University of Washington, Seattle, Washington, USA

[3]Department of Surgery, University of Washington, Seattle, Washington, USA

Correspondence
Nina Isoherranen, Department of Pharmaceutics, University of Washington, Health Science Building, Room H-272M, Box 357610, Seattle, WA 98195-7610, USA.
Email: ni2@uw.edu

Funding information
This work was supported by grants from the National Institutes of Health: 5R01GM111772-06 and 5T32DK007247-42.

Abstract

All-trans-retinoic acid (*at*RA), the active metabolite of vitamin A, has antifibrogenic properties in vitro and in animal models. Liver vitamin A homeostasis is maintained by cell-specific enzymatic activities including storage in hepatic stellate cells (HSCs), secretion into circulation from hepatocytes, and formation and clearance of *at*RA. During chronic liver injury, HSC activation is associated with a decrease in liver retinyl esters and retinol concentrations. *at*RA is synthesized through two enzymatic steps from retinol, but it is unknown if the loss of retinoid stores is associated with changes in *at*RA formation and which cell types contribute to the metabolic changes. The aim of this study was to determine if the vitamin A metabolic flux is perturbed in acute liver injury, and if changes in *at*RA concentrations are associated with HSC activation and collagen expression. At basal levels, HSC and Kupffer cells expressed key genes involved in vitamin A metabolism, whereas after acute liver injury, complex changes to the metabolic flux were observed in liver slices. These changes include a reproducible spike in *at*RA tissue concentrations, decreased retinyl ester and *at*RA formation rate, and time-dependent changes to the expression of metabolizing enzymes. Kinetic simulations suggested that oxidoreductases are important in determining retinoid metabolic flux after liver injury. These early changes precede HSC activation and upregulation of profibrogenic gene expression, which were inversely correlated with *at*RA tissue concentrations, suggesting that HSC and Kupffer cells are key cells involved in changes to vitamin A metabolic flux and signaling after liver injury.

Study Highlights

WHAT IS THE CURRENT KNOWLEDGE ON THE TOPIC?

Vitamin A is metabolized in the liver for storage as retinyl esters in hepatic stellate cell (HSCs) or to *all-trans*-retinoic acid (*at*RA), an active metabolite with antifibrogenic properties. Following chronic liver injury, vitamin A metabolic flux is perturbed, and HSC activation leads to diminished retinoid stores.

WHAT QUESTION DID THIS STUDY ADDRESS?

Do changes in the expression of vitamin A metabolizing enzymes explain changes in *at*RA concentrations and the regulation of fibrosis following acute liver injury?

WHAT DOES THIS STUDY ADD TO OUR KNOWLEDGE?

In healthy liver, both HSC and Kupffer cells may mediate vitamin A homeostasis. Following acute liver injury, complex changes in metabolizing enzyme expression/activity alter the metabolic flux of retinoids, resulting in a transient peak in *at*RA concentrations. The *at*RA concentrations are inversely correlated with profibrogenic gene expression, HSC activation, and collagen deposition.

HOW MIGHT THIS CHANGE CLINICAL PHARMACOLOGY OR TRANSLATIONAL SCIENCE?

Improved understanding of altered vitamin A metabolic flux in acute liver injury may provide insight into cell-specific contributions to vitamin A loss and lead to novel interventions in liver fibrosis.

INTRODUCTION

Vitamin A is a critical dietary nutrient obtained as retinyl esters or pro-vitamin A β-carotene.[1] In enterocytes, retinyl esters are packaged into chylomicrons and trafficked to hepatocytes where they are hydrolyzed to retinol. Retinol is esterified in hepatic stellate cells (HSCs) by the enzyme lethicin-retinol acyltransferase (LRAT), and subsequently stored as retinyl esters in HSC lipid droplets. These depots of retinyl esters account for more than 80% of whole-body vitamin A and are vital for maintaining vitamin A homeostasis. To support the whole-body demand for retinol, retinyl esters are mobilized from storage in HSC and hydrolyzed to retinol, the main circulating form of vitamin A. Retinol circulates bound to the retinol binding protein RBP4, likely complexed in hepatocytes following apo-RBP4 synthesis.[1,2] Numerous enzymes, including lipases and carboxylesterases, contribute to the hydrolysis step.[3] Vitamin A is known to have spatiotemporally regulated metabolism, and retinol may be metabolized to the active metabolite *all-trans*-retinoic acid (*at*RA) in many different cells and tissues to support local signaling.[4,5] Many enzymes, such as retinol dehydrogenases (RDHs) and short chain dehydrogenases (Dhrs), show oxidoreductive activity for reversible retinaldehyde-retinol conversion. In addition, differences in expression levels, co-factor availability, and protein binding may determine the relative roles of these enzymes in the formation of retinaldehyde from retinol.[6,7] Retinaldehyde is further oxidized to *at*RA by aldehyde dehydrogenases, such as ALDH1As.[7] RA clearance, in turn, is predominantly attributed to cytochrome P450 family 26 (CYP26) enzymes, with minor contributions by other CYPs.[8–10]

Vitamin A deficiency has been linked to liver pathology, such as nonalcoholic steatohepatitis (NASH) and nonalcoholic fatty liver disease (NAFLD), and the development of fibrosis. For instance, studies in patients with chronic liver disease and in vitro studies suggest that liver disease is associated with HSC activation, changes in the expression of liver retinoid metabolizing enzymes, such as LRAT, and depletion of hepatic vitamin A.[11–13] In addition, pharmacological use of *at*RA in many rodent models curtails liver fibrogenesis.[14–16] Current evidence links alterations in *at*RA homeostasis and signaling to fibrogenic processes. Specifically, activated HSCs robustly synthesize fibril forming collagens, such as COL1A1 and COL3A1 resulting in tissue scarring,[17–19] and in rodent stellate cells endogenous *at*RA downregulates the mRNA expression of α2(I)collagen through retinoic acid response elements (RAREs) within the promoter region.[20,21] Although other profibrogenic genes possess putative distal RAREs,[22] *at*RA indirectly regulates profibrogenic signals through TGF-β mediated pathways or via upregulation of compensatory signals.[23–28] Based on these findings, we hypothesized that the metabolism of vitamin A is altered in the early stages of liver injury, promoting the antifibrogenic activities of endogenous *at*RA, but vitamin A is subsequently depleted from the liver due to complex changes to the net metabolic flux of vitamin A. The goal of the current study was to determine if retinoid concentrations change due to alterations within the metabolic pathway and if the changes correlate with collagen production using a precision-cut human liver slice model of acute liver injury. In addition, liver cell-specific expression patterns for the vitamin A metabolizing genes were established from human liver donors.

MATERIALS AND METHODS

Human liver tissue and liver slice experiments

Nontumor, virus-free liver tissue came from donors undergoing liver resection at the University of Washington Medical Center. All patients in this study prospectively consented to donate liver tissue for research under the institutional review board. Samples from resected tissue were collected as core biopsies (6 mm in diameter) for liver slice preparations or as a wedge for cell sorting.

Liver cores were cut into 250-μm-thick slices using a vibrating microtome (Leica VT1200 S). Day 0 slice samples were immediately fixed for histology or stored at −80°C for

mRNA quantification or retinoid measurements. The remaining slices were cultured as previously described.[29] For time course experiments, slices from five donors were used for retinoid measurements, slices from two donors for mRNA quantification of profibrogenic genes, and a subset of vitamin A related genes and slices from a minimum of three donors were used for histological staining. Slices and culture media were sampled in duplicates or triplicates at $t = 0.5$, 1, 2, 4, and 7 days unless otherwise stated. For time course experiments, retinoid measurements for donor 1 slices included samples at 10 and 15 days, whereas donor 5 was sampled only up to 4 days. Slices fixed for histology were sampled at 2 and 7 days. Detailed experimental methods for slicing, culturing, and mRNA quantification are in Supplementary Methods.

The temporal changes in metabolic activity (formation of retinyl palmitate-d_6 and *at*RA-d_6 from retinol-d_6) were measured in cultured liver slices from one donor. The medium was analyzed by liquid-chromatography tandem mass spectrometry (LC-MS/MS) as the incubation starting concentration and the assays were initiated by adding 2 μM (media concentration) retinol-d_6 at $t = 0$, 12, or 44 h of culture and triplicate media and slices were sampled at $t = 4$, 16, or 48 h. Retinyl acetate and acitretin were added as internal standards and retinoids quantified by LC-MS/MS.

Isolation of liver cell populations, mRNA expression, and histology

To isolate human liver cells, liver tissue wedges were perfused with collagenase, dissociated, and filtered through sterile mesh. Strained filtrate was centrifuged to separate hepatocytes from nonparenchymal cells, and a Percoll gradient was applied to both fractions to improve purity of the isolated cells. The isolated nonparenchymal cell mixture was stained with an antibody cocktail for cell-sorting using flow cytometry. Pelleted hepatocytes and sorted cells were stored at −80°C prior to RNA extraction. RNA was isolated, converted to cDNA, and analyzed with a 48 × 48 dynamic array and a BioMark HD microfluidics system (Fluidigm, San Francisco, CA). For histology, liver slices were fixed using 10% neutral-buffered formalin, embedded in paraffin, and sliced into 4-μm-thick sections, and stained using trichrome stain, picrosirius red stain, and alpha-smooth muscle actin stain. Detailed experimental procedures are described in Supplementary Methods.

Quantification of vitamin A metabolome

Liver slices were preweighed and homogenized under yellow-lights in 720 μL saline using a handheld homogenizer and disposable soft-tissue OmniTip plastic homogenizing probe (Omni International). Homogenates were transferred to glass borosilicate tubes on ice, spiked with internal standard mixture, and retinol, retinyl esters, and retinoic acid were extracted using a two-round liquid-liquid extraction protocol, as previously described.[30] Culture media was protein precipitated with acetonitrile (1:3), centrifuged at 16,000 × g for 15 min and supernatants collected for analysis. LC-MS/MS analysis of retinoids was performed as previously described using an AB Sciex 6500 QTRAP mass spectrometer (AB Sciex LLC) coupled with Shimadzu UFLC XR DGU-20A5 (Shimadzu Corp.).[30] Analytes were monitored using the multiple reaction monitoring (MRM) transitions: m/z 269 > 93,95 (retinol and retinyl palmitate); m/z 277 > 98, 102 (retinol-d_8); m/z 275 > 98,102 (retinol-d_6 and retinyl palmitate-d_6); m/z 273 > 94,98 (retinyl palmitate-d_4); m/z 269 > 93 (retinyl acetate); 301 > 205 (*at*RA); m/z 307 > 211 (*at*RA-d_6); m/z 327 > 177 (Acitretin). Analyte peaks were integrated against a standard curve using Multiquant.

Kinetic modeling of vitamin A metabolic flux

A kinetic model of the vitamin A metabolic flux in liver slices (normalized to 1 mg liver tissue) was constructed using MATLAB and Simulink platform (R2018a; MathWorks) and established based on known metabolic pathways for vitamin A in human liver involving retinyl palmitate, retinol, retinaldehyde, and *at*RA (Figure S1). All model parameters are summarized in Table S1, and all governing equations and model development and verification steps are described in Supplementary Material. The baseline rate constants of the kinetic model were verified by comparing the simulated concentration ratios to observed whole liver retinoid concentration ratios from an independent dataset[11] (Figure S2). To define the potential changes in enzyme activities that could explain the observed time-dependent changes in retinoid concentrations in human liver slices over 96-h culture, the individual enzyme expressions/activities were altered in a stepwise manner based on known regulation and alterations in primary retinoid metabolizing enzymes as described in Supplementary Material. In time course simulations for endogenous retinoids, experimentally determined mean baseline retinoid concentrations in liver slices were used as initial conditions at $t = 0$ and the simulations were conducted for 96 h. The disposition of retinyl palmitate-d_6, retinol-d_6, and *at*RA-d_6 in the slices was simulated via dosing 20 pmol retinol-d_6 and allowing the metabolism to proceed for 4 h, using the simulated midpoint enzyme expression/activity value at 2-h, 14-h, and 46-h post-slicing as constant parameters. The MATLAB model file and a representative code script are included as Supplementary Material.

RESULTS

HSC activation and upregulation of fibrogenesis-associated genes in human liver slices

To test whether the previously described[29] wound-repair signals promote fibrogenesis in liver slice cultures, temporal changes in liver histology and transcriptional regulation were assessed in cultures maintained for up to 15 days. At day 0, histological staining indicated minimal scarring or collagen deposition (Figure 1a). Alpha smooth muscle actin (α-SMA) was expressed in the periportal regions, with minimal staining outside of portal-tract region (Figure 1a). Slices from 2-day cultures had observable deposition of collagen with more pronounced α-SMA staining in the portal tract, suggestive of initial wound response and extracellular matrix (ECM) reorganization. After 7 days in culture, there was robust collagen deposition and fibrin formation in the liver slices, and α-SMA expression was diffuse throughout the slice, indicative of HSC activation and differentiation to myofibroblasts. These histological changes correlated with transcriptional changes indicative of HSC activation. After 48 h of culture, as collagen deposition and wound response became apparent, expression of profibrotic genes *COL1A1* (Figure 1b), *COL3A1* (Figure 1c), and *TIMP-1* (Figure 1d) were significantly increased in two separate donors, in line with previous findings.[29] The expression levels further increased with culture time corresponding to the collagen deposition and fibrogenesis. However, during the first 12–24 h in culture, the expression of fibrogenic genes was either unchanged or decreased corresponding to the lack of scarring or changes in α-SMA in the early time points of culture.

Temporal changes to vitamin A metabolism

Based on the antifibrogenic role of *at*RA, it was hypothesized that the temporal changes of profibrogenic genes early in culture correlate with changes in *at*RA concentrations. To test this, retinoid concentrations were measured over 4–15 days in liver slices from 5 donors. At baseline, *at*RA concentrations were 0.01–0.045 pmol/mg (Figure 2; Table S2). The baseline concentrations of retinyl palmitate (27–1250 pmol/mg) and retinol (1.1–23 pmol/mg) were highly variable between donors (Table S2). The tissue concentrations of *at*RA spiked at 12 h in all donors (2–95-fold increase compared to baseline), with the *at*RA concentrations being significantly greater ($p = 0.0313$) at 12 h compared with baseline (Figure 2). This spike was followed by a rapid decline in slice *at*RA concentrations by 48 h and throughout culture. The acute spike in *at*RA concentrations at 12 h corresponded to the substantial decrease in the collagen genes' expression (Figure 1b–d). Similarly, the subsequent decline in *at*RA concentrations corresponded to the increase in collagen gene expression. Despite the consistent changes in *at*RA concentrations and collagen gene expression, retinyl palmitate and retinol concentrations did not consistently change with time in the liver slices or in the media (Figure S3). Yet, the subjects with the greatest change in *at*RA concentrations at 12 h also had the highest retinol concentrations, whereas the subjects with the smallest increase had the lowest. The media concentrations of *at*RA were unchanged for the first 48 h followed by a decrease in media *at*RA concentrations over prolonged culture.

The concentration of *at*RA is controlled by a complement of metabolic enzymes, which are regulated by variety of environmental factors and by *at*RA concentrations. As such, we hypothesized that the temporal changes in *at*RA concentrations resulted from altered metabolic enzyme activities during culture. To test this, retinol-d_6 metabolism was measured in liver slices at different time points in culture. The formation rate of retinyl palmitate-d_6 and *at*RA-d_6 was decreased at 12–16 h of culture and further decreased at 44–48 h in comparison to the first 4 h, clearly demonstrating altered vitamin A metabolism in the liver slices over the course of fibrogenesis. No differences were observed in media or slice retinol-d_6 concentrations (Figure 3).

To further explore whether the changes in retinol esterification were related to altered enzyme expression, the time course of *LRAT, RBP4, CRBP1*, and *STRA6* mRNA expression was assessed (Figure S4). *LRAT* mRNA decreased rapidly in the first 24 h of culture (Figure S4a) corresponding to the observed decrease in retinyl palmitate-d_6 formation. *RBP4* and *CRBP1* mRNA also decreased in the first 24 h. Expression of *CRBP1* recovered and was increased by 48 h whereas *RBP4* mRNA stayed extremely low throughout culture (Figure S4c,d). Expression of *STRA6*, encoding the retinol uptake transporter, increased throughout the time course (Figure S4b).

Liver cell-type-specific basal expression of vitamin A metabolic pathway genes

To explore which cell type in the liver may be driving the changes in retinoid metabolism over the course of slice culture, the expression of vitamin A metabolizing genes was determined in isolated liver cell types from six donors (Figure 4). As expected, *LRAT* was expressed predominantly in HSCs with no expression observed in hepatocytes, total nonparenchymal cells (NPCs) or liver sinusoidal endothelial cells (LSECs). Surprisingly, LRAT mRNA was clearly expressed in $CD32^{+high}$ Kupffer cells (KCs).[31] Transcripts of the binding protein *RBP4* were observed in hepatocytes and HSC, but not clearly detected in LSECs or KCs. The intracellular retinol binding protein *CRBP1* was expressed in hepatocytes, LSECs, HSCs, and

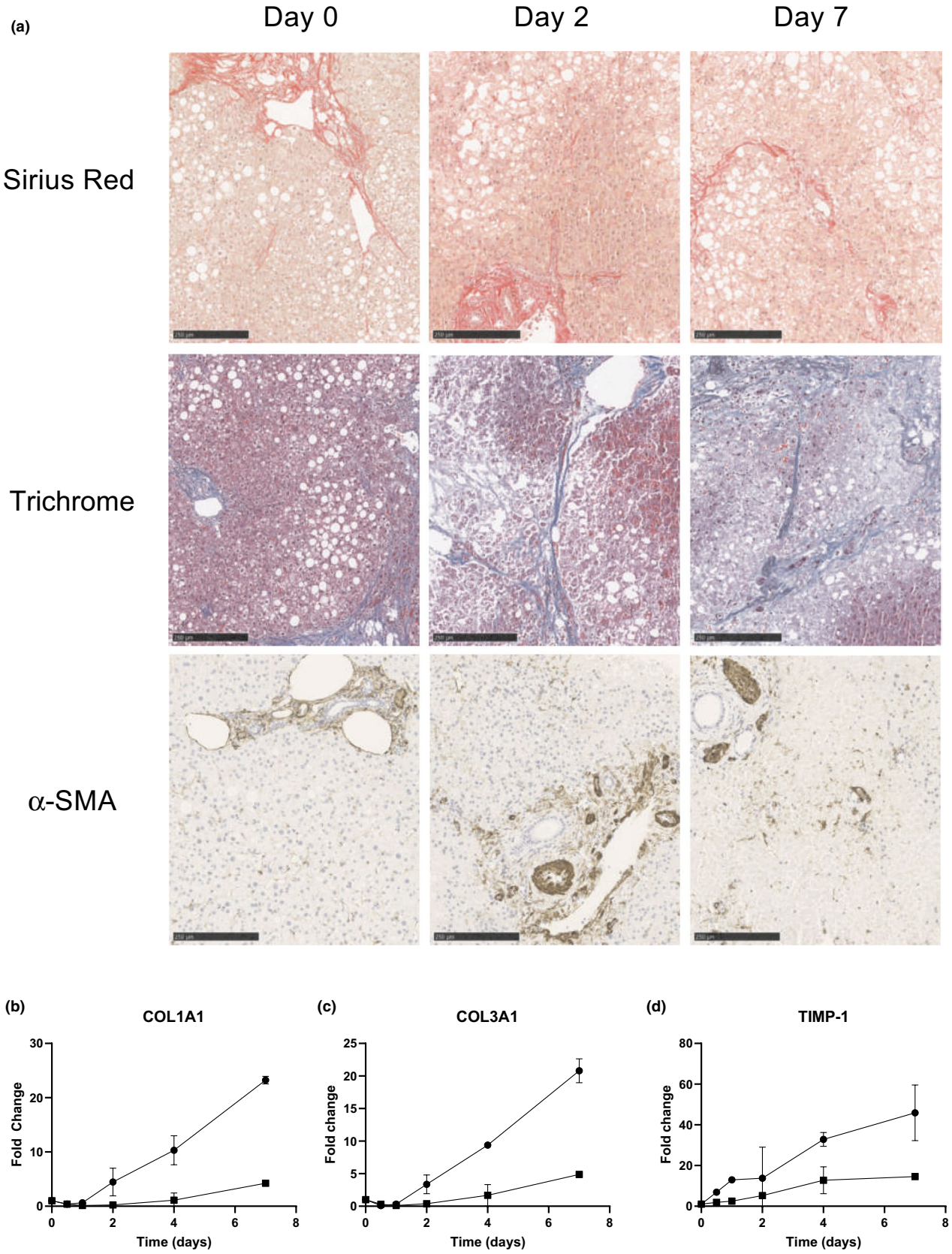

FIGURE 1 Human liver slice cultures as a model for liver fibrogenesis. Human liver slices were cultured up to 15 days on inserts and collagen deposition was assessed in fixed slices with Sirius Red (a; top row) and Trichrome staining (a; middle row). The onset of fibrogenesis was further assessed by staining for alpha-smooth muscle actin, a marker of hepatic stellate cell activation (a, bottom row). Histological panels are shown at 25× magnification with scale bars equal to 250 μm. The time course of the mRNA expression of key fibrogenic genes *COL1A1* (b), *COL3A1* (c), and *TIMP-1* (d) was assessed in slices from two donors in 1–3 replicate slices per time point and data are shown as mean and range

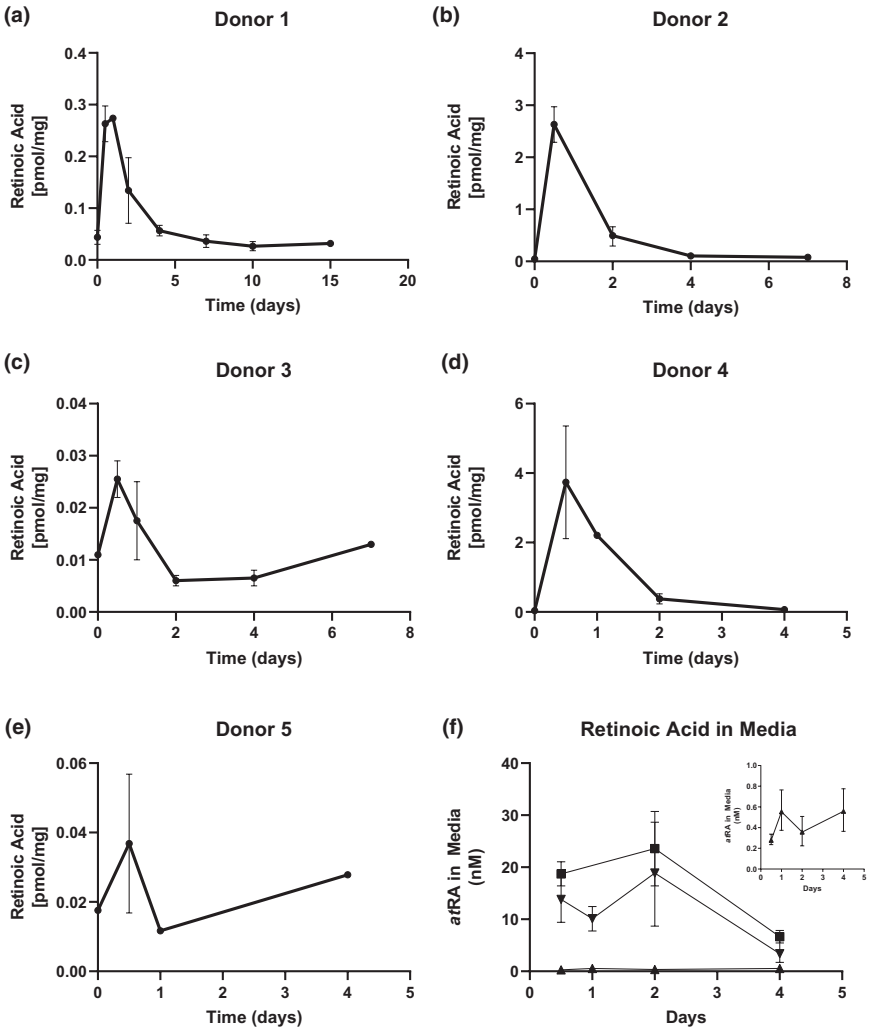

FIGURE 2 Retinoic acid concentration-time course profile during liver slice culturing. Human liver slices were cultured on Transwell plates. Slices and media samples were taken on $t = 0$, 12, 24, 48, 96, and 168 h (for 2 subjects only) and the vitamin A metabolites were quantified using LC-MS/MS. Concentrations in slices were normalized to the slice weight in mg. The full-time course of retinoic acid tissue concentrations is shown for individual liver donors (a–e) as well as for media concentrations for three donors (f). The inset of panel f shows one donor on different scale. All data are shown as mean ± SD. *at*RA, *all-trans*-retinoic acid; LC-MS/MS, liquid-chromatography tandem mass spectrometry

CD32^{+high} KCs. Surprisingly *STRA6* mRNA, indicative of uptake of RBP4-bound retinol from circulation, was below the threshold of detection in the whole liver and in hepatocytes. Yet robust, although variable, STRA6 expression was detected in HSCs and CD32^{+high} KCs. Expression of both *ALDH1A1* and *ALDH1A2*, the two retinaldehyde dehydrogenases that are believed to be the rate-limiting enzymes in *at*RA synthesis, was observed in all livers albeit with distinctly different expression patterns. *ALDH1A1* was broadly expressed but most robustly expressed in hepatocytes. *ALDH1A2*, on the other hand, was expressed in LSECs and HSCs. *ALDH1A2* mRNA was also detected in KCs when sorted based on the magnitude of CD32 expression (Figure 4).

Basal *at*RA is cleared predominantly by CYP26A1 in the liver, but the localization of CYP26A1 in the liver is unknown. *CYP26A1* transcript expression was high in HSCs in 4 donors, whereas all 6 subjects had detectable, but low expression of CYP26A1 in hepatocytes (Figure 4). In addition, CYP26A1 was measured in CD32^{+high} KCs from 2 donors. Notably, *LRAT*, *CYP26A1*, and *ALDH1A2* all share a similar expression pattern in HSCs and CD32^{+high} KCs, which may be due to a requisite role in maintaining vitamin A homeostasis in the liver and retinoid signaling in these cell types. The relationships among major enzyme expression, function, and liver cell types are summarized in Figure 5.

Several liver enzymes in addition to the canonical vitamin A metabolic pathway enzymes have activity toward hepatic retinoid oxidation and the cell-type specific mRNA expression of some of these enzymes was also measured. Aldehyde oxidase (*AOX*) was detectable in whole liver and hepatocytes in all subjects, in HSCs for 4 subjects, and in CD32^{+high} KCs in 2 subjects (Figure 4). *CYP1B1*, a potential retinaldehyde synthesizing enzyme, was expressed at low levels in the whole liver, hepatocytes, LSECs, HSCs, and KCs of all subjects, whereas *ADH7* was expressed in HSC and CD32^{+high} KCs. CYP2C8 and CYP3A4 oxidize *at*RA, and transcripts of both were abundant in whole liver, hepatocytes, and HSCs. The fatty acid binding protein *FABP1* was expressed in HSCs and hepatocytes unlike albumin (*ALB*), which was observed in all liver cell-types (Figure 4).

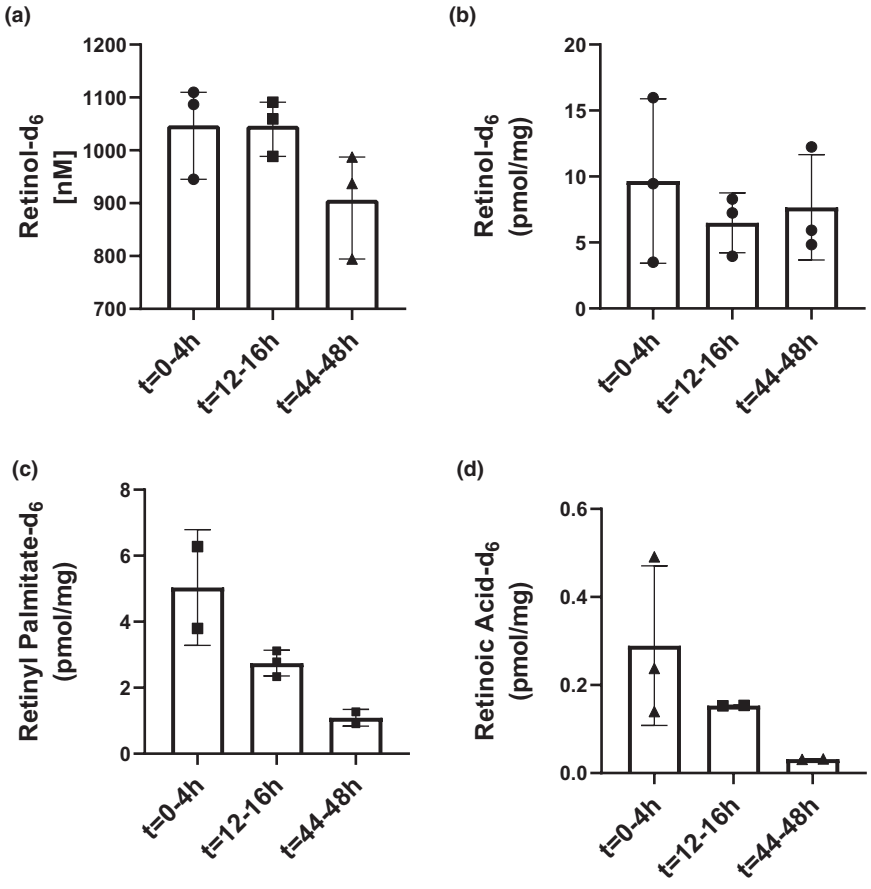

FIGURE 3 Retinol-d_6 metabolism in human liver slices. Human liver slices were prepared from a single donor and cultured on Transwell plates. At 0, 12, and 44 h in culture, slice media was replaced with growth media supplemented with 2 μM retinol-d_6. Media and slices were sampled 4 h later at $t = 4$, 24, and 48 h, respectively. Retinoids were quantified to determine the media concentration of retinol-d_6 at the end of the 4 h treatments (a), and the concentration of retinol-d_6 (b), retinyl palmitate-d_6 (c) and *all-trans*-retinoic acid-d_6 (d) in the slices at the end of the 4 h treatments. The measured concentrations are shown as mean ± SD of technical triplicates and the concentrations shown are normalized to the initial media concentration of retinol-d_6. *at*RA, *all-trans*-retinoic acid

Kinetic modeling of vitamin A metabolic flux

To explore potential metabolic processes that result in the time-dependent changes in retinoid concentrations in cultured liver slices, and to define whether the detected changes in enzyme expression could result in the observed changes in retinoid concentrations, a kinetic model of vitamin A metabolic flux was developed (Figure S1; Table S1). Simulations were then performed to test the impact of perturbations in specific activities on the liver retinoid metabolic flux and concentrations. Decrease in LRAT expression/activity alone resulted in a modest decrease in liver retinyl esters and elevation in liver retinol and *at*RA concentrations (Figure 6). When a decrease in LRAT activity was combined with CYP26 induction, liver *at*RA concentrations were predicted to decrease, whereas retinol and retinyl palmitate concentrations were unaffected. Neither of these scenarios, while supported by experimental data, could replicate the observed spike in *at*RA concentrations. Yet, when changes in retinol oxidation and retinaldehyde reduction (RDH and Dhrs mediated pathways) were incorporated into the simulations, the spike in *at*RA concentrations and the lack of change in other retinoids could be simulated (Figure 6), suggesting that the time course of retinoid concentrations in the liver slices is a result of changes in multiple enzymes' activities. This model was further tested via simulation of the changes in retinol-d_6 metabolism with time (Figure 7). Consistent with the endogenous retinoid modeling, reduction of the activity/expression of LRAT with or without CYP26 induction (Figure S5) alone did not explain the decrease in formed retinyl palmitate-d_6 or *at*RA-d_6 concentrations. Likewise, the iterative additions of reduced retinal reductase activity, reduced retinol oxidation, and induction of alternative retinol clearance pathway failed to fully recapitulate the decrease in *at*RA formation rate (Figure 7). However, the observed data could be simulated by decreasing the baseline retinal reductase activity (Figure 7, Figure S5) further supporting the conclusion that retinol oxidation and retinal reduction play key roles in regulating temporal changes in liver *at*RA concentrations. When the simulation included a reduction in retinol oxidation, a minor increase in retinol concentrations was observed suggesting the alternative elimination/secretion of retinol must be increased. Collectively, these simulations suggest that retinal reduction and retinol oxidation drive the observed spike in *at*RA concentrations.

DISCUSSION

All-trans-retinoic acid (*at*RA) is a multifaceted signaling molecule that may mediate liver fibrogenesis. For example, *at*RA has been shown to repress collagen expression

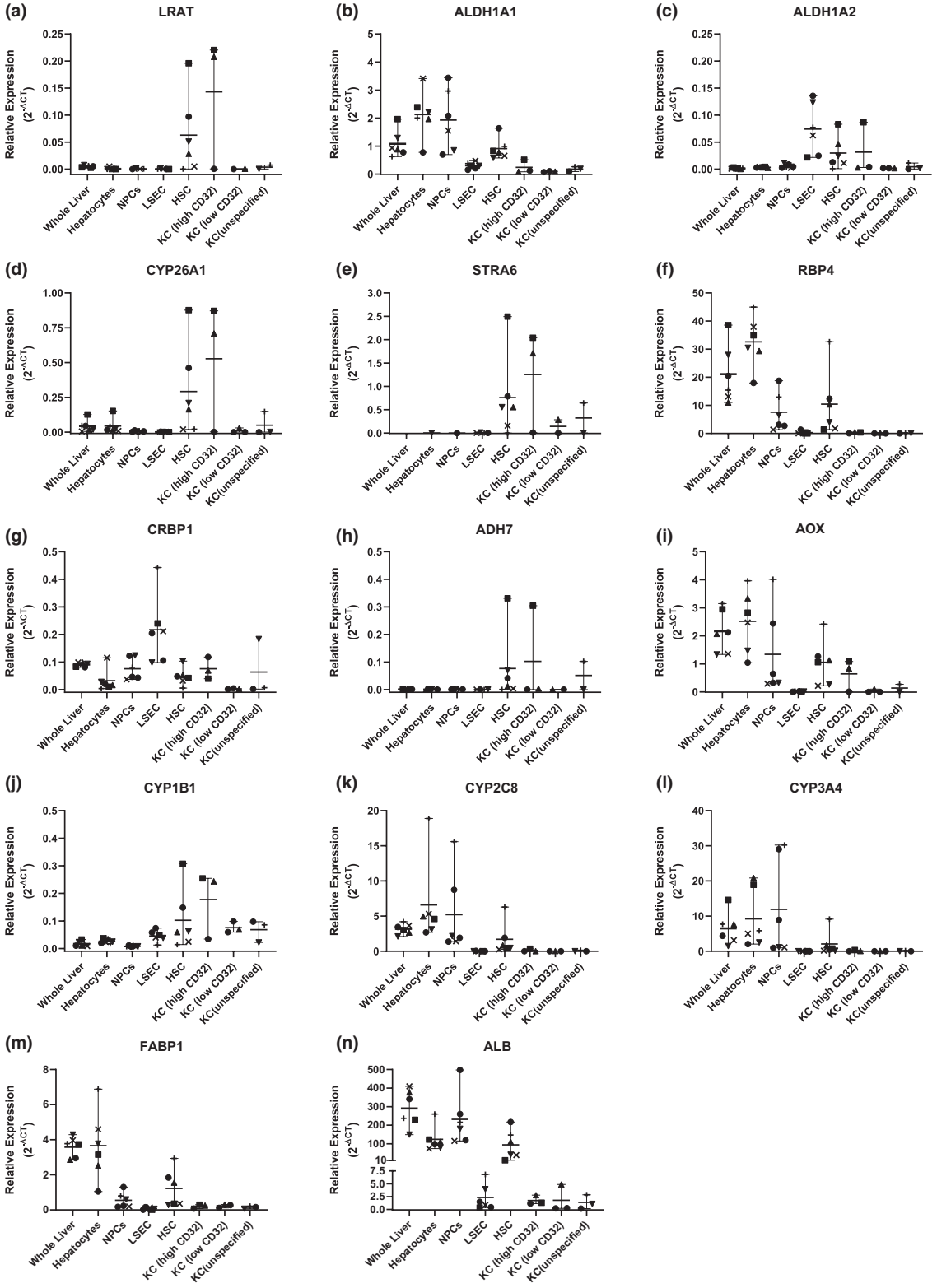

FIGURE 4 Expression of genes encoding vitamin A metabolizing enzymes and binding proteins in different liver cell types. Human liver samples ($n = 6$) were dissociated using collagen perfusion, and hepatocytes were separated from non-parenchymal cells using density centrifugation. NPCs were stained with fluorescent antibodies towards liver cell-type specific markers and sorted into RNA-later using flow cytometry. Total RNA was extracted from each liver sample and gene expression quantified using Fluidigm system. Data was normalized to the average gene expression of three housekeeping genes: *ACTB*, *GAPDH*, and *HPRT1* and expressed as "Relative Abundance" using the delta CT method. Data is shown as individual $2^{-\Delta CT}$ with the mean and range. ALB, albumin; AOX, aldehyde oxidase; KC, Kupffer cell; LRAT, lethicin-retinol acyltransferase; NPC, nonparenchymal cell

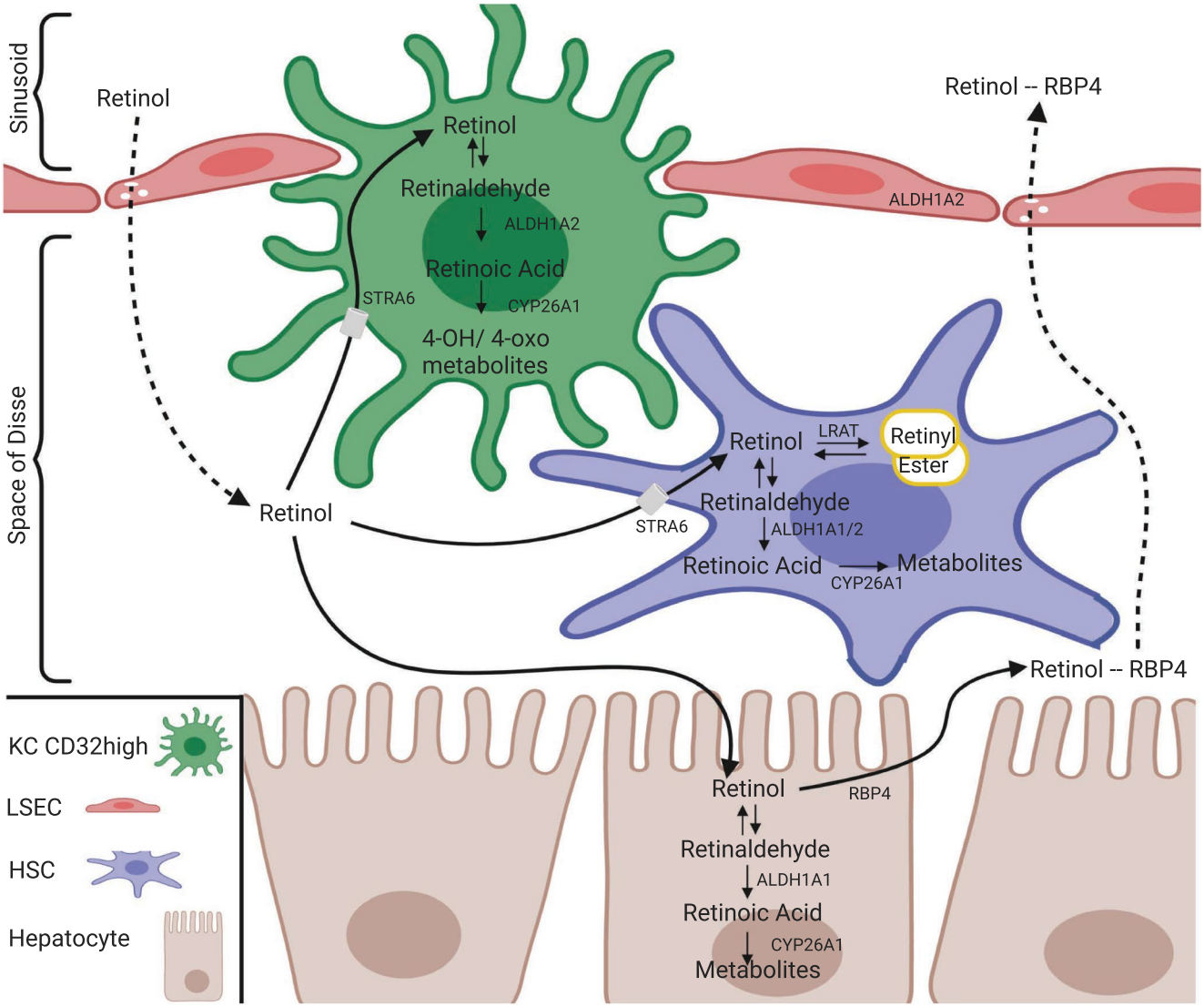

FIGURE 5 Inferred basal vitamin A metabolic pathways in individual human liver cell types. Using the cell-type-specific enrichment of vitamin A metabolizing enzymes and binding proteins, proposed metabolic pathways for vitamin A are shown for each cell type. The data confirm the key role of HSCs, but also show that KCs are equipped to play a major role in all aspects of vitamin A metabolism, except for storage as retinyl esters. Image created with BioRender.com. HSC, hepatic stellate cell; KC, Kupffer cell; LSEC, liver sinusoidal endothelial cell

in mice,[20,21] and block profibrogenic signaling by TGF-β via multiple indirect mechanisms.[16,27] Yet, the role of *at*RA signaling in human liver fibrogenesis has not been established. The results shown here from precision cut human liver slice cultures suggest that *at*RA liver concentrations peak within the first 24 h after an acute liver injury and that retinoid metabolizing enzymes in the HSC, and possibly KC, may mediate this early response and the time-course of fibrogenesis. Changes to retinoid metabolic enzyme expression and activity were found to precede HSC activation and collagen upregulation. Kinetic simulations of the vitamin A metabolic flux support the interpretation that the early peak of *at*RA concentrations is a result of carefully orchestrated changes in the enzymatic activities of multiple enzymes in the vitamin A metabolic pathway. Together, the data support a strong link among altered *at*RA concentrations, vitamin A metabolism, and liver fibrogenesis.

The current study demonstrates that *at*RA signaling is preferentially localized in HSC following liver injury and that early changes in *at*RA formation and/or clearance may result in a delay in HSC activation, α-SMA mRNA expression, and collagen deposition. Within the first 12 h after liver injury, *at*RA concentrations reproducibly and significantly peaked in every donor despite variability in the basal retinoid concentrations, suggesting *at*RA signaling may be a core element in the response to injury. HSCs are vital contributors to both the wound-repair and fibrosis process, although many different liver cell types are involved in acute liver injury.[32] This implies that early changes in HSC result in retinoid-mediated signaling effects on other liver cells.

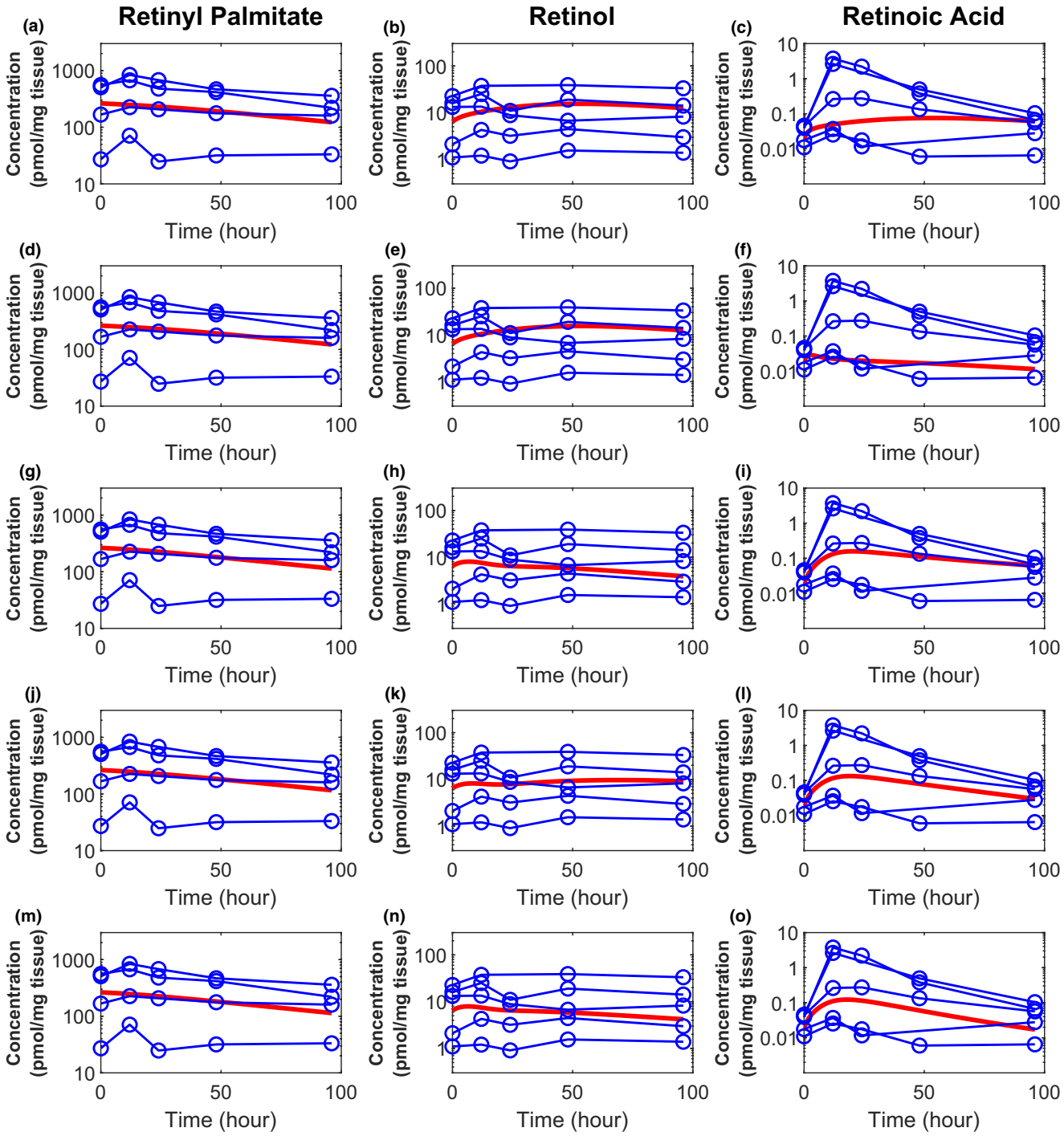

FIGURE 6 Simulations of time-dependent changes of endogenous retinoids (retinyl ester, retinol, and *at*RA) in human liver slices using the developed retinoid flux model. The simulations show five different scenarios of changes in enzymatic activities: (1) LRAT expression/activity is decreased (a–c); (2) LRAT expression/activity is decreased and CYP26 expression is induced (d–f); (3) LRAT and retinal reductase expression/activity are decreased and CYP26 expression is induced (g–i); (4) LRAT, retinal reductase, and retinol oxidase expression/activity are decreased and CYP26 expression is induced (j–l); and (5) LRAT, retinal reductase, and retinol oxidase expression/activity are decreased and CYP26 and retinol additional elimination pathway are induced (m–o). The observed data from experiments in individual donors are shown in blue open circles. The simulation results are shown in red solid curves. The left, middle, and right columns show endogenous retinyl ester, retinol, and *at*RA respectively. *at*RA, *all-trans*-retinoic acid; LRAT, lethicin-retinol acyltransferase

Recent anatomic evidence supports the idea that KCs interact intimately with HSCs, LSECs, and hepatocytes, forming a complex niche that favors cross-talk between all major liver cell types.[33] This close contact favors the transmission of an array of paracrine signals promoting KC activation, hepatocyte proliferation, and tissue reorganization.[32–34] In

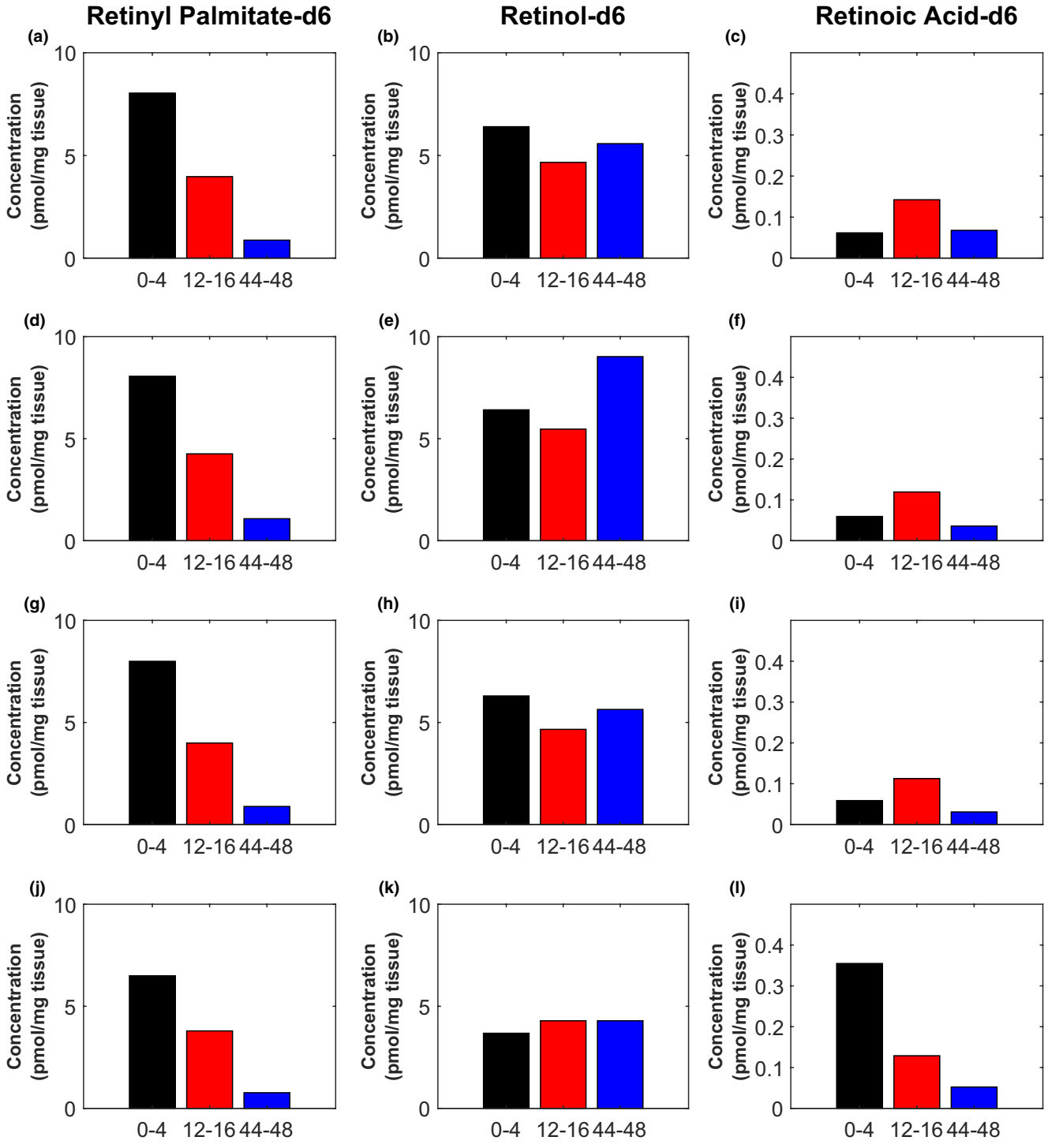

FIGURE 7 Simulations of d_6-labeled retinoid (retinyl ester, retinol, and *at*RA) concentrations in human liver slices. The concentrations shown are the simulated values at the end of 4 h of culture after dosing retinol-d_6 at 0 h (shown in black), 12 h (shown in red), and 44 h (shown in blue) post-slicing using the developed retinoid flux model in four different scenarios: (1) LRAT and retinal reductase expression/activity were decreased and CYP26 expression was induced (a–c); (2) LRAT, retinal reductase, and retinol oxidase expression/activity were decreased and CYP26 expression was induced (d–f); (3) LRAT, retinal reductase, and retinol oxidase expression/activity were decreased and CYP26 and retinol additional elimination pathways were induced (g–i); and (4) LRAT expression/activity were decreased and CYP26 and retinol additional elimination pathway was induced, the baseline retinal reductase expression/activity was assumed to be low, and both retinal reductase and retinol oxidase expression/activity remain constant (j–l). The left, middle, and right columns show d_6-labeled retinyl ester, retinol, and *at*RA, respectively. The simulation results of additional scenarios of enzyme expression/activity level are shown in Figure S3. *at*RA, *all-trans*-retinoic acid; LRAT, lethicin-retinol acyltransferase

lieu of termination of the wound repair process, activated HSCs may trans-differentiate into myofibroblasts. Such myofibroblasts produce an excess of fibril forming type I and III collagens, which are deposited in the Space of Disse and constitute fibrosis.[32,34] HSC activation is also strongly associated with the loss of retinoid stores from lipid droplets.[13] However, surprisingly, no significant changes in the total liver retinyl ester or retinol concentrations were observed in the current study. This finding may reflect the complex changes to the metabolic pathway and binding proteins during the acute phase response and the size of the retinyl ester reserves in the liver slices.[5]

At basal levels, the results indicate that HSCs have a dominant role and can mediate every step in the metabolic pathway maintaining vitamin A homeostasis. This is supported by extensive literature evidence implicating HSCs as central in retinoid metabolism.[1,13] However, a novel finding of this study is that KCs are also equipped to play a major role. Notably, both HSCs and KCs expressed the mRNA for ADH7, one of many RDH and Dhrs enzymes involved in the reversible formation and reduction of retinaldehyde. The results from this study also suggest that hepatocytes provide minimal contribution to basal vitamin A homeostasis, *at*RA biosynthesis, and clearance, but are important for maintaining circulating retinol concentrations. Collectively, these findings suggest that HSCs, and possibly a subset of KCs, are critical for maintaining vitamin A metabolic homeostasis in the liver.

After the acute liver injury resulting from slicing, retinoid metabolism was altered. A previous study in rodents showed that secretion of IL-1α by KCs postinjury activates stellate cells, downregulates *LRAT* mRNA expression, and reduces liver retinyl ester stores. In the current study, *LRAT* mRNA expression rapidly decreased post-slicing, whereas the formation rate of retinyl palmitate-d_6 from retinol-d_6 was decreased. This is in agreement with previous findings.[13] Within the first 16 h, the apparent formation of *at*RA-d_6 from retinol-d_6 was also reduced. This is supported by data from 2 liver slice studies suggesting *CYP26A1* is induced by 24 h[35] and after 5 days in culture.[36] However, based on the kinetic modeling, decrease in LRAT expression and induction of CYP26A1 are not sufficient to explain the time-dependent changes in vitamin A metabolic flux. Although there are no data on the impact of liver disease on the various RDH and Dhrs enzyme expression or activity, *ALDH1A1* and *ALDH1A2* were previously found to be upregulated at 5 days,[36] but not in 24-h cultures.[35] This data together with our modeling suggests that the spike in *at*RA concentrations cannot be explained by changes in ALDH1A activity.

The simulations of vitamin A metabolic flux indicate that a key component driving changes in *at*RA concentrations is change in RDH and/or Dhrs activity after injury. In addition, a decrease in retinol esterification and increase in *at*RA clearance appear to be important for modulating *at*RA concentrations and signaling after liver injury. Retinol oxidation is considered the overall rate-limiting step in *at*RA biosynthesis, although many enzymes have been attributed to this reversible reaction and the predominant enzymes involved in the liver are not clear.[6,7] Recent literature evidence has suggested that RDHs and Dhrs may work cooperatively to facilitate higher catalytic rates.[37] Specifically, RDH10 and the *at*RA-inducible Dhrs3 form a higher order protein complex, and cooperatively work to maintain steady-state retinaldehyde levels and slow *at*RA formation to prevent excess *at*RA formation.[6,37,38] The simulations presented here collectively incorporate these enzymatic processes but the developed kinetic model does not have the sensitivity to differentiate between RDH and Dhrs activity and cooperativity. In addition, retinoid binding protein changes or cofactor availability cannot be ruled out by the data in the current study as causes for altered enzyme activity.[6,7] Overall, the simulations emphasize the need for defining the role of specific oxidoreductases in vitamin A homeostasis in the liver, in response to acute liver injury and association with HSC activation.

In conclusion, HSC and a subset of KC are responsible for vitamin A metabolism in the liver, and likely responsible for the acute elevation of *at*RA liver concentrations. The *at*RA may protect the liver from profibrogenic HSC activities, but its effects are transient due to complex changes in vitamin A metabolism. These findings suggest that re-establishing vitamin A homeostasis following the wound repair process may prevent the development of liver fibrosis, and that pharmacological use of retinoids may be beneficial in liver injury. Future experiments are needed to quantify the changes in protein expression of retinoid metabolizing enzymes and determine if expression correlates with retinoid concentrations and/or the degree of fibrosis in patients with liver injury. In addition, pharmacological interventions to combat vitamin A dysregulation following liver injury should be explored for its potential to promote liver regeneration and delay fibrogenic processes.

DISCLAIMER

As Associate Editor of *Clinical & Translational Science*, Nina Isoherranen was not involved in the review or decision process for this paper.

CONFLICT OF INTEREST

N.I. holds a US Patent 9963439 on novel Cyp26 inhibitors. All other authors declared no competing interests for this work.

AUTHOR CONTRIBUTIONS

L.C., N.H., W.H., I.C., and N.I. wrote the manuscript. X.W., L.C., I.C., and N.I. designed the research. X.W., L.C., N.H.,

W.H, and J.R. performed the research. L.C., X.W., I.C., and N.I. analyzed the data. J.R., H.K., and R.Y contributed new reagents/analytical tools.

REFERENCES

1. Blaner WS, Li Y, Brun PJ, Yuen JJ, Lee SA, Clugston RD. Vitamin A Absorption, Storage and Mobilization. M Asson-Batres, C Rochette-Egly, In: *The Biochemistry of Retinoid Signaling II. Sub-Cellular Biochemistry*, Vol. 81. New York, NY: Springer; 2016:95-125.
2. Achkar CC, Derguini F, Blumberg B, et al. 4-Oxoretinol, a new natural ligand and transactivator of the retinoic acid receptors. *Proc Natl Acad Sci USA*. 1996;93:4879-4884.
3. Chelstowska S, Widjaja-Adhi MAK, Silvaroli JA, Golczak M. Molecular basis for vitamin A uptake and storage in vertebrates. *Nutrients*. 2016;8:676.
4. Blaner WS. Vitamin A signaling and homeostasis in obesity, diabetes, and metabolic disorders. *Pharmacol Ther.* 2019;197:153-178.
5. Li Y, Wongsiriroj N, Blaner WS. The multifaceted nature of retinoid transport and metabolism. *Hepatobiliary Surg Nutr.* 2014;3:126-139.
6. Belyaeva OV, Adams MK, Popov KM, Kedishvili NY. Generation of retinaldehyde for retinoic acid biosynthesis. *Biomolecules*. 2020;10:5.
7. Kedishvili NY. Retinoic acid synthesis and degradation. *Subcell Biochem*. 2016;81:127-161.
8. Thatcher JE, Zelter A, Isoherranen N. The relative importance of CYP26A1 in hepatic clearance of all-trans retinoic acid. *Biochem Pharmacol*. 2010;80:903-912.
9. Isoherranen N, Zhong G. Biochemical and physiological importance of the CYP26 retinoic acid hydroxylases. *Pharmacol Ther*. 2019;204:107400.
10. Ross AC, Zolfaghari R. Cytochrome P450s in the regulation of cellular retinoic acid metabolism. *Annu Rev Nutr.* 2011;31:65-87.
11. Zhong G, Kirkwood J, Won KJ, Tjota N, Jeong H, Isoherranen N. Characterization of Vitamin A metabolome in human livers with and without nonalcoholic fatty liver disease. *J Pharmacol Exp Ther*. 2019;370:92-103.
12. Pettinelli P, Arendt BM, Teterina A, et al. Altered hepatic genes related to retinol metabolism and plasma retinol in patients with non-alcoholic fatty liver disease. *PLoS One*. 2018;13:e0205747.
13. Kida Y, Xia Z, Zheng S, et al. Interleukin-1 as an injury signal mobilizes retinyl esters in hepatic stellate cells through down regulation of lecithin retinol acyltransferase. *PLoS One*. 2011;6:e26644.
14. Senoo H, Wake K. Suppression of experimental hepatic fibrosis by administration of vitamin A. *Lab Investig*. 1985;52:182-194.
15. Panebianco C, Oben JA, Vinciguerra M, Pazienza V. Senescence in hepatic stellate cells as a mechanism of liver fibrosis reversal: a putative synergy between retinoic acid and PPAR-gamma signalings. *Clin Exp Med*. 2017;17:269-280.
16. Ye Y, Dan Z. All-trans retinoic acid diminishes collagen production in a hepatic stellate cell line via suppression of active protein-1 and c-Jun N-terminal kinase signal. *J Huazhong Univ Sci Technol Med Sci*. 2010;30:726-733.
17. Higashi T, Friedman SL, Hoshida Y. Hepatic stellate cells as key target in liver fibrosis. *Adv Drug Deliv Rev*. 2017;121:27-42.
18. Friedman SL. Hepatic stellate cells: Protean, multifunctional, and enigmatic cells of the liver. *Physiol Rev*. 2008;88:125-172.
19. Khomich O, Ivanov AV, Bartosch B. Metabolic hallmarks of hepatic stellate cells in liver fibrosis. *Cells*. 2019;9:24.
20. Wang L, Tankersley LR, Tang M, Potter JJ, Mezey E. Regulation of α2(I) collagen expression in stellate cells by retinoic acid and retinoid X receptors through interactions with their cofactors. *Arch Biochem Biophys.* 2004;428:92-98.
21. Wang L, Rennie LT, Tang M, Potter JJ, Mezey E. Regulation of the murine α2(I) collagen promoter by retinoic acid and retinoid X receptors. *Arch Biochem Biophys.* 2002;401:262-270.
22. Lalevée S, Anno YN, Chatagnon A, et al. Genome-wide in Silico identification of new conserved and functional retinoic acid receptor response elements (direct repeats separated by 5 bp). *J Biol Chem.* 2011;286:33322-33334.
23. Zhong C, Pu L, Fang M, Rao J, Wang X. ATRA regulates innate immunity in liver ischemia/reperfusion injury via RARα/Akt/Foxo1 signaling. *Biol Pharm Bull*. 2018;41:530-535.
24. Dutta A, Sen T, Chatterjee A. All-trans retinoic acid (ATRA) downregulates MMP-9 by modulating its regulatory molecules. *Cell Adhes Migr*. 2010;4:409-418.
25. Sierra-Mondragon E, Rodríguez-Muñoz R, Namorado-Tonix C, et al. All-trans retinoic acid attenuates fibrotic processes by downregulating tgf-β1/smad3 in early diabetic nephropathy. *Biomolecules*. 2019;9:525.
26. Wang H, Dan Z, Jiang H. Effect of all-trans retinoic acid on liver fibrosis induced by common bile duct ligation in rats. *J Huazhong Univ Sci Technol Med Sci*. 2008;28:553-557.
27. Hisamori S, Tabata C, Kadokawa Y, et al. All-trans-retinoic acid ameliorates carbon tetrachloride-induced liver fibrosis in mice through modulating cytokine production. *Liver Int*. 2008;28:1217-1225.
28. Zhou TB, Drummen GPC, Qin YH. The controversial role of retinoic acid in fibrotic diseases: analysis of involved signaling pathways. *Int J Mol Sci*. 2013;14:226-243.
29. Wu X, Roberto JB, Knupp A, et al. Precision-cut human liver slice cultures as an immunological platform. *J Immunol Methods.* 2018;455:71-79.
30. Czuba LC, Zhong G, Yabut KC, Isoherranen N. Analysis of vitamin A and retinoids in biological matrices. E Pohl, *Methods Enzymol*. New York: Elsevier Inc; 2020;637: 309–340. https://doi.org/10.1016/bs.mie.2020.02.010.
31. Wu X, Hollingshead N, Roberto J, et al. Human liver macrophage subsets defined by CD32. *Front Immunol*. 2020;11. https://www.frontiersin.org/articles/10.3389/fimmu.2020.02108/full.
32. Tanaka M, Miyajima A. Liver regeneration and fibrosis after inflammation. *Inflamm Regen*. 2016;36:1-6.
33. Bonnardel J, T'Jonck W, Gaublomme D, et al. Stellate cells, hepatocytes, and endothelial cells imprint the Kupffer cell identity on monocytes colonizing the liver macrophage niche. *Immunity*. 2019;51:638-654.e9.
34. Karsdal MA, Nielsen SH, Leeming DJ, et al. The good and the bad collagens of fibrosis – their role in signaling and organ function. *Adv Drug Deliv Rev*. 2017;121:43-56.
35. Elferink MGL, Olinga P, Van Leeuwen EM, et al. Gene expression analysis of precision-cut human liver slices indicates stable expression of ADME-Tox related genes. *Toxicol Appl Pharmacol*. 2011;253:57-69.
36. Starokozhko V, Vatakuti S, Schievink B, et al. Maintenance of drug metabolism and transport functions in human precision-cut liver slices during prolonged incubation for 5 days. *Arch Toxicol.* 2017;91:2079-2092.
37. Adams MK, Belyaeva OV, Wu L, Kedishvili NY. The retinaldehyde reductase activity of dhrs3 is reciprocally activated by retinol dehydrogenase 10 to control retinoid homeostasis. *J Biol Chem*. 2014;289:14868-14880.

38. Adams MK, Belyaeva OV, Kedishvili NY. Generation and isolation of recombinant retinoid oxidoreductase complex. E Pohl, In: *Methods in Enzymology*, Vol. 637 New York NY: . New York, NY: Elsevier Inc.; 2020:77-93.

SUPPORTING INFORMATION

Additional supporting information may be found online in the Supporting Information section.

How to cite this article: Czuba LC, Wu X, Huang W, et al. Altered vitamin A metabolism in human liver slices corresponds to fibrogenesis. *Clin Transl Sci*. 2021;14:976–989. https://doi.org/10.1111/cts.12962